Geochemistry Geophysics Geosystems G3
AN ELECTRONIC JOURNAL OF THE EARTH SCIENCES
Published by AGU and the Geochemical Society

Data Brief
Volume 10, Number 5
30 May 2009
Q05011, doi:10.1029/2009GC002440
ISSN: 1525-2027

NA-SWS-1.1: A uniform database of teleseismic shear wave splitting measurements for North America

Kelly H. Liu

Department of Geological Sciences and Engineering, Missouri University of Science and Technology, Rolla, Missouri 65409, USA (liukh@mst.edu)

[1] This version of shear wave splitting (SWS) database (DB) for North America (NA) contains 6224 pairs of splitting parameters (fast polarization directions and splitting times) measured using all the available data recorded by digital broadband seismic stations over the period of 1980–2007 and archived at the Incorporated Research Institutions for Seismology Data Management Center. The measurements were produced using a set of robust procedures that involve automated batch processing and manual screening and were ranked quantitatively on the basis of a uniform criterion. The result is a homogeneous database of individual (rather than station-averaged) splitting parameters that can be used by a variety of geoscientists for the understanding of the structure and dynamics of the Earth's deep interior beneath NA. This data brief describes the seismic data and techniques used to generate the SWS results, the spatial and azimuthal coverage, and the limitations of the DB. The DB will be periodically updated and enhanced by adding newly recorded data and by measuring splitting parameters using the PKS and SKKS phases in addition to SKS. The database can be accessed at http://www.mst.edu/~liukh/SWS.

Components: 4626 words, 10 figures.

Keywords: shear wave splitting; anisotropy; mantle flow; lithosphere; North America; database.

Index Terms: 7208 Seismology: Mantle (1212, 1213, 8124); 7218 Seismology: Lithosphere (1236); 7203 Seismology: Body waves.

Received 16 February 2009; **Revised** 31 March 2009; **Accepted** 3 April 2009; **Published** 30 May 2009.

Liu, K. H. (2009), NA-SWS-1.1: A uniform database of teleseismic shear wave splitting measurements for North America, *Geochem. Geophys. Geosyst.*, *10*, Q05011, doi:10.1029/2009GC002440.

1. Introduction

[2] Seismic anisotropy inferred from measurements of splitting of shear waves generated by distant earthquakes is one of the few ways to measure the strength and direction of mantle fabrics. The most commonly used seismic data are P-to-S converted waves at the core-mantle boundary on the receiver side, including SKS, SKKS, and PKS (see *Silver* [1996], *Savage* [1999], and *Fouch and Rondenay* [2006] for reviews on the theory and practice of shear wave splitting measurements). The major advantage of using XKS phases (which represent all the P-to-S converted phases from the core-mantle boundary) is that at the core-mantle boundary on the receiver side, the P-to-S converted phase is radially polarized. If this shear wave encounters anisotropic material along its path to the receiver, it may split into two different polarizations having different velocities (denoted fast and slow). The splitting parameters are the polarization of the fast shear wave (measured

clockwise from the north) and the travel time difference between the fast and slow shear waves δt. The global average of δt is 1.0 s [*Silver*, 1996].

[3] The major cause of mantle anisotropy is the A-type lattice-preferred orientation (LPO) of olivine [*Jung and Karato*, 2001], which is the main constituent mineral of the upper mantle and is highly anisotropic. Seismic shear waves polarized along the a axis travel faster than those polarized along the b or c axes. Numerical and petrophysical experiments demonstrated that under uniaxial compression, the a axis of olivine turns to be perpendicular to the maximum compressional strain direction; under pure shear, it becomes perpendicular to the shortening direction; and under progressive simple shear, it aligns in the flow direction [*Ribe and Yu*, 1991; *Chastel et al.*, 1993; *Zhang and Karato*, 1995]. Therefore the fast polarization direction for the asthenosphere reflects the flow direction, as observed in ocean basins [*Wolfe and Solomon*, 1998] and continental rifts and passive margins [e.g., *Sandvol et al.*, 1992; *Gao et al.*, 1994, 1997, 2008]. For the lithosphere, ϕ is mostly parallel to the strike of compressional zones, as observed in many places on Earth [*McNamara et al.*, 1994; *Liu et al.*, 1995; *Silver*, 1996; *Barruol and Hoffmann*, 1999; *Fouch and Rondenay*, 2006; *Li and Chen*, 2006].

[4] Shear wave splitting measurements are increasingly used by geodynamic modelers to understand the strength and direction of mantle flow beneath various areas, such as North America [*Fouch et al.*, 2000], the western US [*Becker et al.*, 2006; *Silver and Holt*, 2002], Tibetan Plateau [*Flesch et al.*, 2005; *Wang et al.*, 2008], and the whole globe [*Conrad et al.*, 2007; *Bird et al.*, 2008]. The most popularly used database on a global scale is the one initiated by *Silver* [1996], which is a compilation of about 320 splitting measurements worldwide (about 130 are located in North America) from about 30 studies. Several research groups have since then enriched the database by adding more measurements. Examples of such databases include http://geophysics.asu.edu/anisotropy/upper and http://www.gm.univ-montp2.fr/splitting/DB.

[5] A common feature of these databases is that the results were generated by numerous research groups who used different measuring techniques, and the criteria for data selection and for ranking the results are also different. This resulted in heterogeneous databases. In addition, with few exceptions, the shear wave splitting measurements presented in the currently available databases are station averages. While this is a reasonable approach for areas with simple anisotropy (i.e., a single layer with horizontal axis of symmetry), the average splitting parameters are likely to be misleading for areas with complex anisotropy [*Marone and Romanowicz*, 2007]. This is demonstrated by many studies including our recent identification of significant anisotropy (with a splitting time of up to 1.5 s which is 50% greater than global average) on the southern Tibetan Plateau [*Gao and Liu*, 2009], which is an area that was considered as possessing an isotropic or weakly anisotropic mantle. In addition, most geodynamic modeling studies require distinguishing lithospheric anisotropy and asthenospheric anisotropy [*Conrad et al.*, 2007]. For most continental areas, anisotropy has contributions from both the lithosphere and the underlying asthenosphere. Obviously, it is the asthenospheric anisotropy that is modeled. Because the currently available splitting data sets do not separate lithospheric and asthenospheric contributions to the observed bulk anisotropy, it is virtually impossible to model mantle flow beneath continents by using station averages. This is reflected by the large misfit between the predicted and observed fast directions for stations on continents. A recent study by *Conrad et al.* [2007] found that the misfit between observed station-averaged fast directions and the predicted fast directions is 10° for ocean basins, and is as large as 41° for continents.

[6] This report introduces the first version of a homogeneous shear wave splitting database of 6224 pairs of well-defined (i.e., quality A or B, see section 3.4 below) splitting parameters that we measured over the past several years.

2. Data Sets Used to Construct the Database

[7] The database (DB) uses all the available broadband seismic data archived at the Incorporated Research Institutions for Seismology (IRIS) Data Management Center (DMC), from teleseismic events occurred between 1 January 1980 and 15 March 2007 (Figure 1) for North America and surrounding areas (180°W–50°W, and 0°N–90°N, Figure 2). Data from all the events with an epicentral distance in the range of 81°–140° and a magnitude of 5.6 or larger were obtained from the IRIS DMC. If the focal depth $\geq$100 km, a lower cutoff magnitude of 5.5 was used to take the advantage of sharper

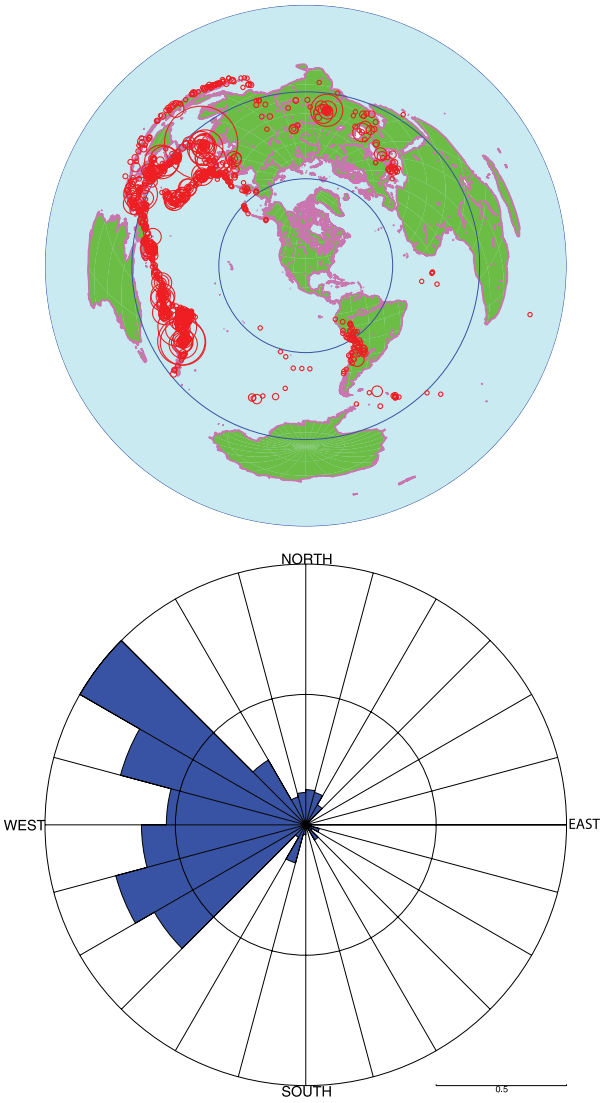

Figure 1. (top) An azimuthal equidistant projection map showing the distribution of earthquakes used in the study. The size of the circles is proportional to the number of quality A and B SKS splitting parameters that the event produced. (bottom) A rose diagram showing the distribution of the back azimuth of the events.

waveforms. The distribution of the earthquakes used in the study is shown in Figure 1. In the study area, a total of 850 stations were found to result in at least one well-defined quality A or B (i.e., quality A or B, see below) SKS measurement (Figures 2 and 3).

[8] The stations belong to either permanent or portable (campaign-style) seismic networks. The networks that contributed the most number of measurements include the Advanced National Seismic System, Global seismic network, Southern and Northern California Seismic Networks, and the USArray.

3. Measuring and Ranking Procedures

[9] The procedures for measuring and ranking splitting parameters consist of several steps (Figure 4), and are a combination of automated processing and manual screening and adjustments.

3.1. Data Requesting and Uniformization

[10] A BREQ_FAST waveform requesting file was generated for each of the stations in the study area using a FORTRAN code. The requested waveform is from 200 s before and 1000 s after the theoretical arrival time (TAT) of the first P or P_{diff} phase computed on the basis of the IASP91 earth model. The seismograms requested are recorded by the broadband and high gain channels (BHN, BHE, and BHZ). The requesting files were then sent by another FORTRAN program using system calls once they were generated. A sufficient time interval (e.g., 1 min) was used between successive file deliveries to avoid overloading the IRIS DMC data requesting system.

[11] The SEED files were fetched using ftp from the DMC once they were generated, and were converted into SAC format using the PASSCAL program *rdseed*. The SAC files are then windowed to start 20 s before and 800 s after the first P or P_{diff} phase. The pre-P or P_{diff} part is used for computing the signal to noise ratio (S/N) in the autoscreening procedure described below. The vertical, north-south, and east-west components from all the stations associated with an event are stored under the same directory named after the event (e.g., EQ070742359 where the first two digits are

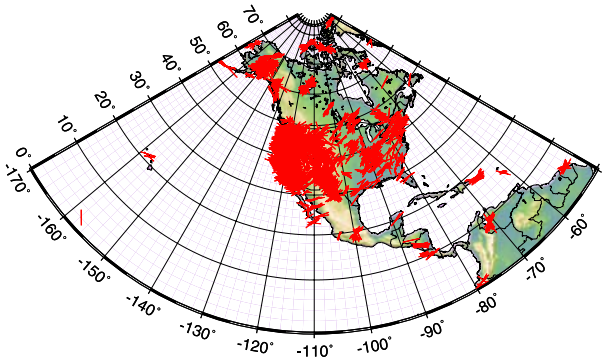

Figure 2. Quality A and B SKS splitting parameters plotted at the surface projection of the ray-piercing points at 200 km depth.

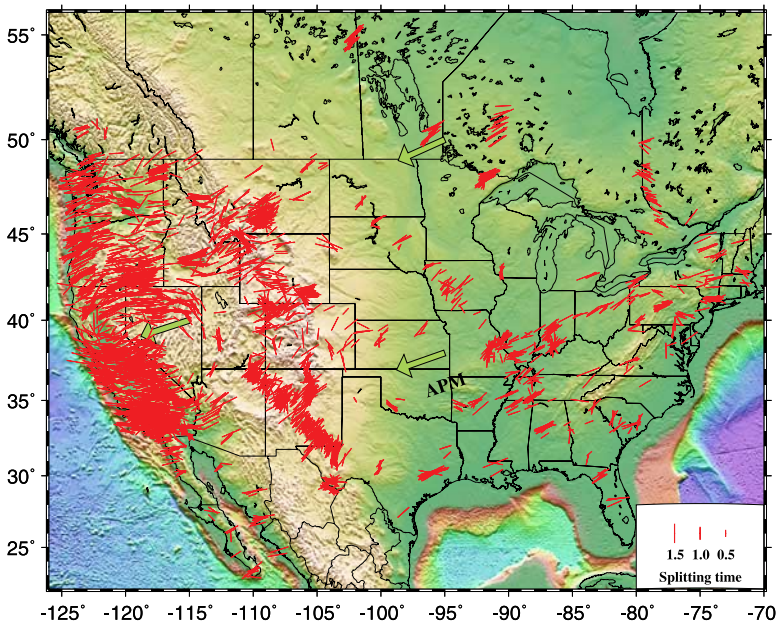

Figure 3. Same as Figure 2 but for the area with dense measurement coverage.

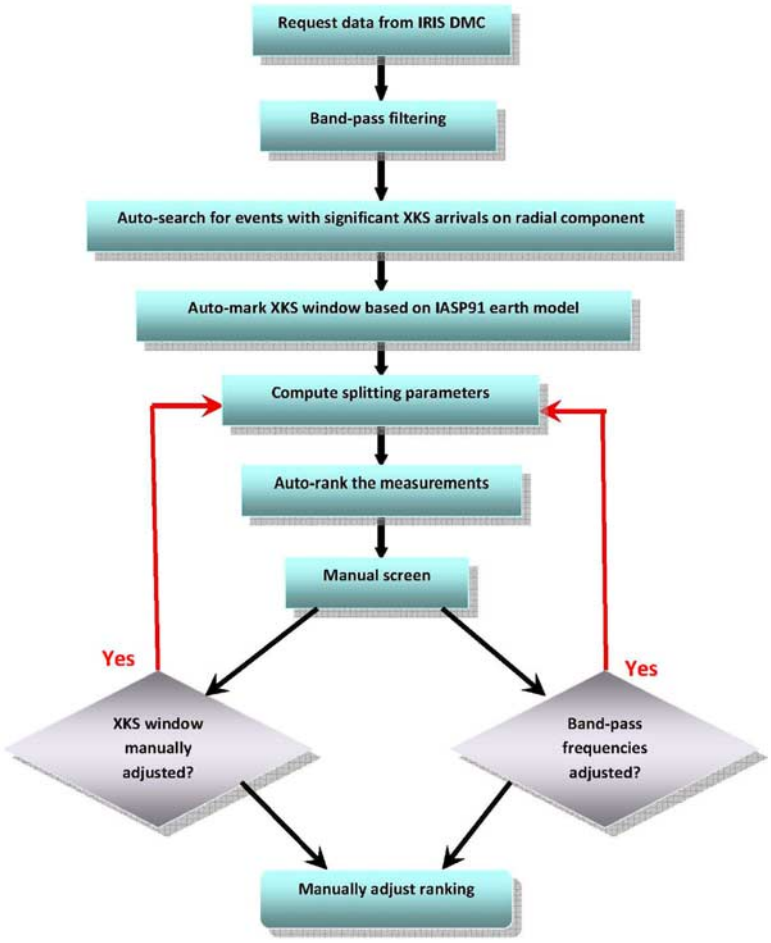

Figure 4. A schematic flowchart showing the procedure for measuring, verifying, and ranking shear wave splitting parameters.

the year, the next 3 digits are the Julian day, followed by the hour and minute of the origin time). Necessary headers including the latitude, longitude, focal depth, and magnitude of the events are added to the SAC files, which are interpolated into a uniform sampling interval of 0.05 s.

3.2. Filtering, Autoscreening, and SKS Arrival Marking

[12] The windowed seismograms were then filtered in the frequency range of 0.04–0.5 Hz using a 4-pole, 2-pass Butterworth filter. The a value which is the beginning time for the SKS window is set as the TAT of the SKS phase, and the f value which is the ending time is set as 5 s before the TAT of the first S or S_{diff} phase if $f - a \leq 30$ s to avoid contamination by the direct S or S_{diff} arrivals, and as $f = a + 30$ s if $f - a \geq 30$ s.

[13] The filtered north-south and east-west components were then gone through an automated screening procedure. An event-station pair is rejected if the signal to noise ratio is smaller than 6.0. The S/N is computed using A_{sks}/A_n where A_{sks} is the maximum value of a time series composed using the north-south($N(t)$) and east-west ($E(t)$) components using $R(t) = \sqrt{N(t)^2+E(t)^2}$ in the time section between a and f, and A_n is the mean absolute value of $R(t)$ in the time window of 3–13 s from the beginning of the time series (which starts 20 s before the TAT of the first P or P_{diff}). A total of 95,935 event-station pairs were selected for further processing. The results of the automated screening procedure was visually checked to ensure that no high-quality SKS traces were excluded.

3.3. Performing SKS Splitting Measurements

[14] The optimal pair of SKS splitting parameters for a given event-station pair is obtained by searching for the one that minimizes the energy on the corrected transverse component [*Silver and Chan*, 1991]. A recent comparative study [*Vecsey et al.*, 2008] found that among the several commonly used shear wave splitting methods, the minimization of transverse energy approach is the most stable one. The errors in the resulting splitting parameters can be calculated using the inverse F test and represent the 95% confidence level (and are thus approximately 2 standard deviations) [*Silver and Chan*, 1991].

3.4. Quantitative Ranking of the Measurements

[15] To obtain a well-defined pair of parameters, a high S/N is required in both the radial and transverse component, which in turn requires a strong anisotropy and a significant difference between the back azimuth of the event and the fast direction. Another requirement is that SKS energy on the transverse component should be adequately removed after the optimal parameters are applied. On the basis of these criteria, we proposed an objective ranking procedure to divide the measurements into five categories including [*Liu et al.*, 2008].

[16] A means outstanding. For a quality A measurement, outstanding energy on both the radial and transverse components is observed, and the measuring program was effective in reducing the energy on the transverse component. Figure 5 shows an example of quality A measurement.

[17] B means good. Seismograms used to obtain measurements in this category are similar to those in A, but with lower S/N on the radial component. Figure 6 shows an example of quality B measurement.

[18] N means null. The null measurements are the results of weak anisotropy, weak presplitting SKS energy, the SKS phase arriving from a direction that is close to the fast or slow directions, or a combination of the factors above. Our results show that the vast majority of the null measurements are the result of weak presplitting SKS energy and the fact that many earthquakes arrive from the west (Figure 1) which is close to the dominantly E-W fast polarization direction observed at many stations in North America (NA). Because of these ambiguities and our goal of only providing well-defined measurements in the first version of the DB, null results are not presented.

[19] S means special. For measurements in this category, good or outstanding SKS arrivals can be observed on both the original radial and transverse components, but the energy on the corrected transverse component cannot be effectively reduced. This could be the results of complex anisotropy, scattering, and/or misorientation of the sensors, as recently suggested by *Liu et al.* [2008] for a station in Mongolia.

[20] C means unusable. A pair of measurements are considered as unusable if the S/N on the original radial component is small. Some of the measurements with quality A, B, or S are not well

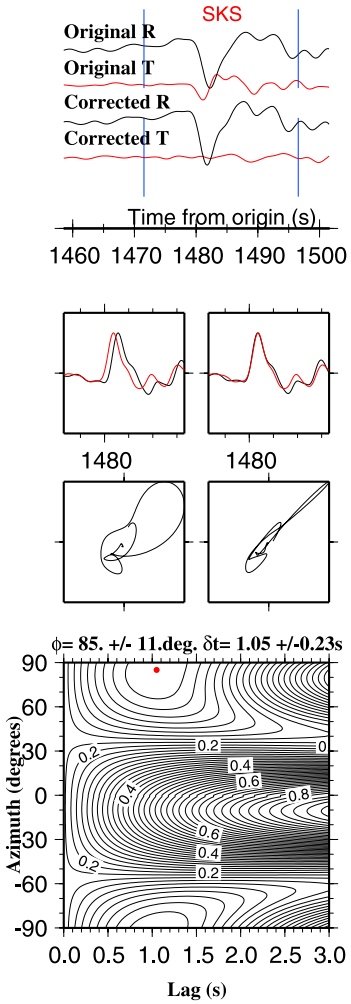

Figure 5. Original and corrected radial and transverse components, their particle motion patterns, and the error function for a quality A measurement. Shown at the bottom are quantities used to rank the measurements. R_{or}, R_{ot}, and R_{ct} are the S/N on the original radial, original transverse, and the corrected transverse components, respectively. Details about the quantities and the ranking procedure are given by *Liu et al.* [2008].

constrained as suggested by the large errors in ϕ or δt or both. Those measurements are also given a quality of C if $\sigma_\phi > 20°$ or $\sigma_{\delta t} > 1.0$ s.

3.5. Manual Screening

[21] To ensure that the automatically measured and ranked results are reliable, all the measurements went through a time-consuming manual screening process. Three groups of parameters are checked and if necessary, are modified. The first is the *a* and *f* values of the SKS time window used for measurement. They are adjusted if significant non-SKS arrivals are in the SKS window. The second group of parameters that are checked and adjusted is the band pass filtering parameters. This is useful for removing strong noise within the default 0.04–0.5 Hz band. As shown in the flowchart (Figure 4), when one or more of the above parameters are adjusted, the event-station pair is remeasured and reranked. Finally, the ranking is manually adjusted if necessary to more accurately reflect the quality of the measurements.

4. Major Characteristics of the DB

[22] The procedure above produced 1229 quality A, 4995 quality B, 15913 quality N, and 1109 quality S measurements. The rest of the measurements belong to quality C. Understandably, none of the events with an epicentral distance smaller than 83° resulted in quality A or B measurements due to the small separation between the SKS and S phases.

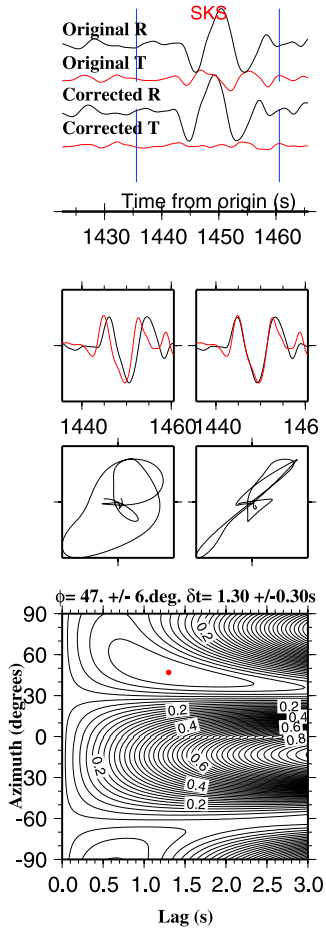

Figure 6. Same as Figure 5 but for a quality B measurement.

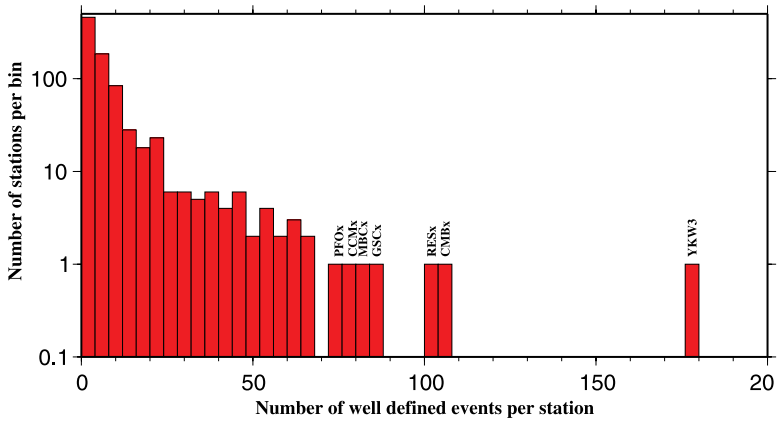

Figure 7. A histogram showing the number of quality A and B measurements per station. Note the logarithmic scale of the vertical axis.

The individual splitting measurements that plotted above the ray-piercing points at 200 km depth are shown in Figures 2 and 3. For the 850 stations that have at least one quality A or B measurements, about 2/3 of them have 5 or less measurements, and seven of the stations (YKW3, CMB, RES, GSC, MBC, CCM, and PFO) have 75 or more quality A or B measurements (Figure 7).

4.1. Columns of the Database

[23] Column 1 gives the station. This field contains the name of the station as it appears in the IRIS DMC. Please note that if the name has less than 4 letters, one or more lowercase x's are added at the end of the name so that all the stations have 4-letter names which are convenient for most computer applications. A "summary plot" (see Figure 8 for an example) for all the measurements from a station shows up when the user clicks on the station name.

[24] Column 2 gives the event. The events are named as EQyydddhhmm where yy is the year, ddd is the Julian day, hh is the hour, and mm is the minute of the origin time (Universal time).

[25] Columns 3 and 4 give station latitude and longitude in degrees.

[26] Columns 5 and 6 give the fast polarization direction (measured clockwise from the north) and its 2σ marginal uncertainty in degree.

[27] Columns 7 and 8 give splitting time and its 2σ marginal uncertainty in second.

[28] Column 9 gives BAZ, which is the back azimuth of the event relative to the station measured clockwise from the north.

[29] Column 10 gives BAZ90, which is the modulo-90° of BAZ. BAZ90 = BAZ when BAZ $\in$ (0, 90), BAZ90 = BAZ-90 when BAZ $\in$ (90, 180), BAZ90 = BAZ-180 when BAZ $\in$ (180, 270), and BAZ90 = BAZ-270 when BAZ $\in$ (270, 360). BAZ90 is particularly useful for modeling anisotropic structures with a $\pi/2$ periodicity such as two horizontal layers [*Silver and Savage*, 1994].

[30] Columns 11, 12, and 13 give the latitude and longitude (in degree) of the epicenter and the depth (in km) of the focus.

[31] Columns 14 gives quality rank.

[32] Columns 15 and 16 give the latitude and longitude of the SKS ray-piercing points, computed at a depth of 200 km.

[33] Column 17 gives a plot of the original and corrected radial and transverse components, the particle motion patterns, and the error function for the event. See Figures 5 and 6 for examples.

4.2. Spatial Distribution of the Measurements

[34] The spatial distribution of the ray-piercing points is quantified by computing the radius of circles that contain 20 A or B measurements. The center of the circles is 0.2° apart. The results (Figure 9) suggest that the western US orogenic zone has the highest, and the rest of the areas have much lower coverage density except for a few "hot spots" such as the New Madrid seismic zone. The arrival of the USArray to the central and eastern US will significantly improve the spatial coverage.

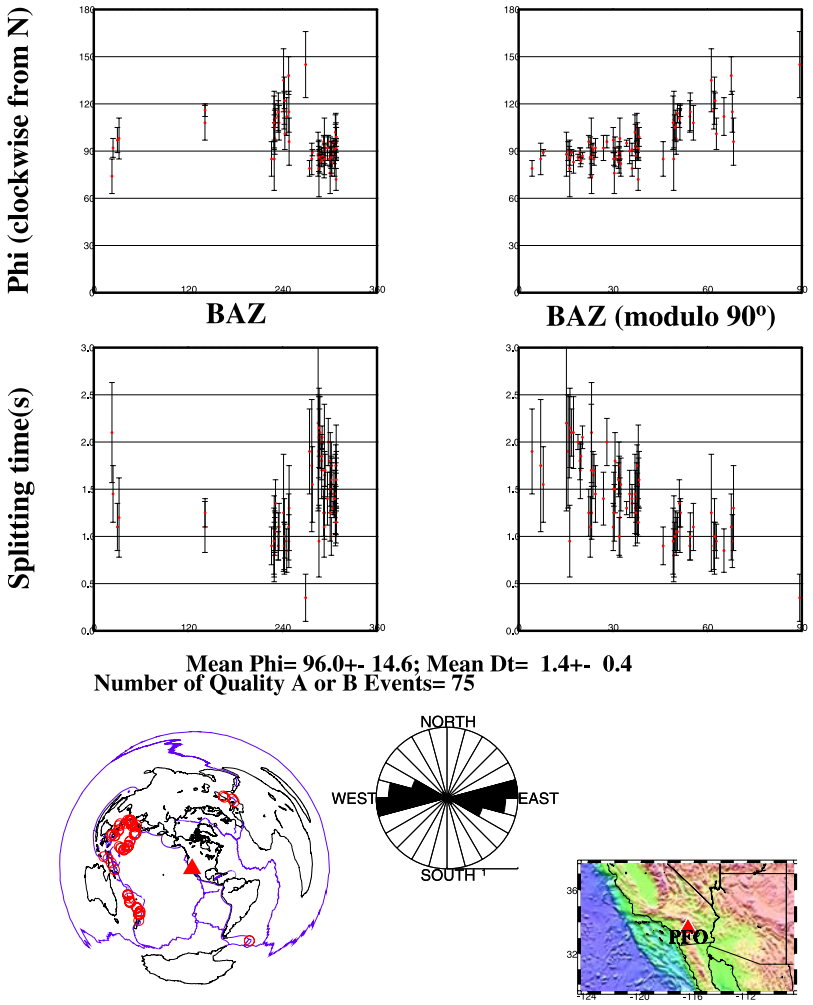

Figure 8. Azimuthal variations of (top) ϕ and (middle) δt and (bottom) distribution of events and rose diagram of ϕ measurements for station PFO.

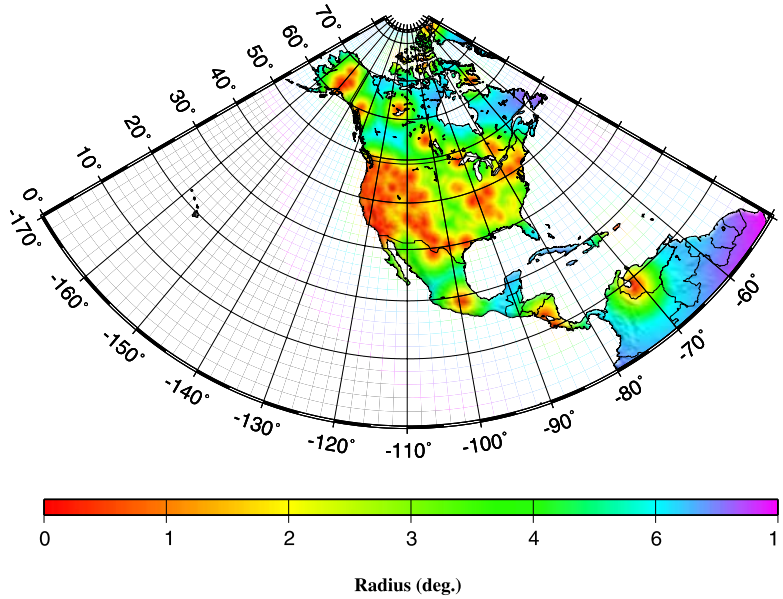

Figure 9. Distribution of the radius of circles containing 20 quality A or B measurements.

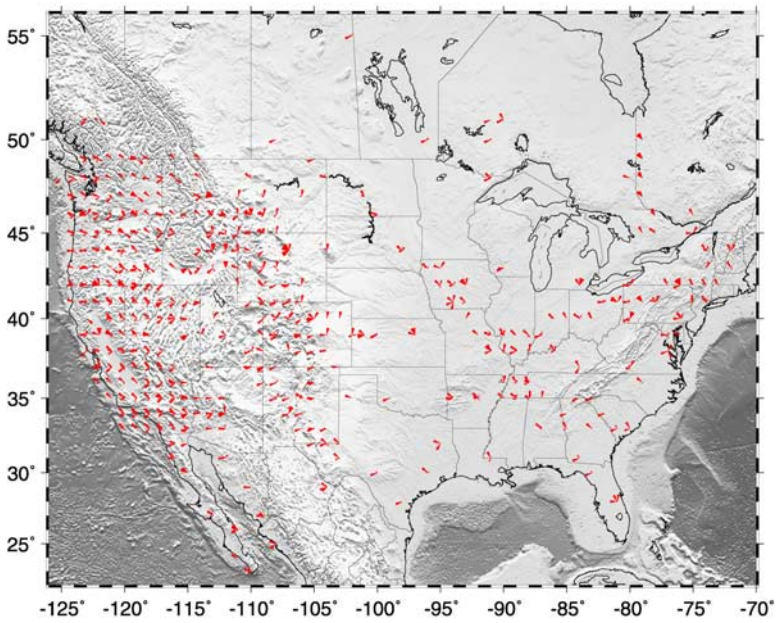

Figure 10. Rose diagrams showing the distribution of back azimuth in 1° by 1° blocks for the area with the majority of SKS splitting measurements.

4.3. Azimuthal Coverage of the Measurements

[35] The majority of the events have a back azimuth in the 90° range of 225–315° (Figure 1), suggesting a high feasibility of resolving two-layer anisotropy which is characterized by a $\pi/2$ periodicity, as demonstrated by the measurements on station PFO in southern California (Figure 8). To explore the spatial variation in azimuth coverage, a rose diagram is generated for each of the 1° by 1° blocks (Figure 10). The plot is informative for some studies that require events from a certain azimuth.

5. Limitations of the DB and Future Plans for Development

[36] Like many other databases, the shear wave splitting (SWS) DB has an intrinsically evolving nature and has a number of areas that can be enhanced by additional work.

[37] The first limitation of the DB is that it uses only the SKS phase. As demonstrated by a recent study using data from station LSA on the Tibetan Plateau [*Gao and Liu*, 2009], the addition of PKS and SKKS results could dramatically increase the azimuthal coverage and consequently the resolving power of the splitting measurements on complex anisotropy. We have developed and tested our procedure for making PKS and SKKS splitting measurements on the basis of the SKS procedure and plan to add results from PKS and SKKS to future versions of the database.

[38] The next limitation is that most of the stations only have a limited number of measurements (Figure 7). This is obviously due to the fact that many of the stations belong to campaign-style experiments or the USArray which has a 2-year duration of deployment, and some of the permanent stations were recently established. Addition of new data sets recorded since 15 March 2007 will certainly increase the number of measurements per station for the permanent stations. In addition, adding PKS and SKKS measurements will most likely double the number of measurements at most stations.

[39] The third limitation is that the seismograms were filtered using a single frequency band. It has been realized that at least beneath some areas such as New Zealand, the splitting parameters especially the splitting times are frequency-dependent [*Savage*, 1999]. Such dependence can be revealed by performing shear wave splitting measurements using seismograms filtered in a series narrow frequency bands, although such filtering will likely reduce the S/N of the signal. We will explore the feasibility of measuring and presenting results in a few frequency bands in future versions.

[40] The fourth limitation of the database is the very uneven spatial coverage (Figure 9). The

ongoing USArray will certainly improve the spatial coverage, although the western US orogenic zone will most likely be the area with the highest density of splitting measurements for a long time to come.

[41] The last limitation of the database concerns its structure and searchability. The current database is a simple HTML table. While it is manageable by most users because of its relatively small size, future versions will be searchable ones based on a number of criteria such as latitude and longitude of a region, back azimuth, and earthquake location and depth to better serve researchers with various applications of the database.

[42] It should be mentioned that in spite of the limitations mentioned above, the present version of the DB was established using data and procedures that are similar in nature to the vast majority of previous SWS studies, which used only the SKS phase and its entire frequency contents.

6. Summary

[43] Using a uniform procedure for data requesting, shear wave splitting parameter measurement and ranking, a homogeneous database of SKS splitting parameters for North America was created using all the available broadband seismic data archived at the IRIS DMC prior to early 2007. Relative to existing shear wave splitting databases which are mostly compilations of published results by numerous research groups using different measuring techniques and ranking criteria, NA-SWS-1.1 is unique in the spatial coverage, homogeneity in measuring techniques, ranking criteria, and feasibility for future development. Consequently, it is expected that it will be an important resource for geoscientists especially geodynamic modelers to use the shear wave splitting measurements as constrains to the models, for structural geologists to relate surface structural features with deeper structures, for petrologists to understand source of fabrics in mantle xenoliths, and for seismologists to use the database as references in planning higher-resolution shear wave splitting and other studies and to remove receiver-side anisotropy to study source-side anisotropy and anisotropy in the lower mantle and the core of the Earth.

Acknowledgments

[44] Data used in the study were archived and managed by the IRIS DMC. S.S. Gao helped with the development of the SWS measurement procedure. I thank P. Bird, K. Fischer, S. Gao, T. Lay, B. Romanowicz, D. Schutt, P. Silver, R. Stern, H. Yuan, and many others in the seismological and geodynamic communities for their encouragement at various occasions to produce a uniform SWS database. This study is supported by NSF award EAR-0739015 entitled "Testing the hypothesis of pervasive two-layer azimuthal anisotropy beneath North America" and by the University of Missouri Research Board award UMRB-3569 entitled "A systematic shear-wave splitting measurement procedure."

References

Barruol, G., and R. Hoffmann (1999), Upper mantle anisotropy beneath the Geoscope stations, *J. Geophys. Res.*, *104*, 10,757–10,773.

Becker, T. W., V. Schulte-Pelkum, D. K. Blackman, J. B. Kellogg, and R. J. O'Connell (2006), Mantle flow under the western United State from shear wave splitting, *Earth Planet. Sci. Lett.*, *247*, 235–251.

Bird, P., Z. Liu, and W. K. Rucker (2008), Stresses that drive the plates from below: Definitions, computational path, model optimization, and error analysis, *J. Geophys. Res.*, *113*, B11406, doi:10.1029/2007JB005460.

Chastel, Y. B., P. R. Dawson, H. R. Wenk, and K. Bennett (1993), Anisotropic convection with implications for the upper mantle, *J. Geophys. Res.*, *98*, 17,757–17,771.

Conrad, C. P., M. D. Behn, and P. G. Silver (2007), Global mantle flow and the development of seismic anisotropy: Differences between the oceanic and continental upper mantle, *J. Geophys. Res.*, *112*, B07317, doi:10.1029/2006JB004608.

Flesch, L. M., W. E. Holt, P. G. Silver, M. Stephenson, C. Y. Wang, and W. W. Chan (2005), Constraining the extent of crust-mantle coupling in central Asia using GPS, geologic, and shear wave splitting data, *Earth Planet. Sci. Lett.*, *238*(1–2), 248–268.

Fouch, M. J., and S. Rondenay (2006), Seismic anisotropy beneath stable continental interiors, *Phys. Earth Planet. Inter.*, *158*, 292–320.

Fouch, M. J., K. M. Fischer, and E. M. Parmentier (2000), Shear wave splitting, continental keels, and patterns of mantle flow, *J. Geophys. Res.*, *105*(B3), 6255–6275.

Gao, S. S., and K. H. Liu (2009), Significant seismic anisotropy beneath the southern Lhasa Terrane, Tibetan Plateau, *Geochem. Geophys. Geosyst.*, *10*, Q02008, doi:10.1029/2008GC002227.

Gao, S. S., P. M. Davis, K. H. Liu, P. D. Slack, Y. A. Zorin, V. V. Mordvinova, V. M. Kozhevnikov, and R. P. Meyer (1994), Seismic anisotropy and mantle flow beneath the Baikal rift zone, *Nature*, *371*, 149–151.

Gao, S. S., P. M. Davis, K. H. Liu, P. D. Slack, A. W. Rigor, Y. A. Zorin, V. V. Mordvinova, V. M. Kozhevnikov, and N. A. Logatchev (1997), SKS splitting beneath continental rift zones, *J. Geophys. Res.*, *102*, 22,781–22,797.

Gao, S. S., K. H. Liu, R. J. Stern, G. R. Keller, J. P. Hogan, J. Pulliam, and E. Y. Anthony (2008), Characteristics of mantle fabrics beneath the southern-central United State: Constraints from shear-wave splitting measurements, *Geosphere*, *4*, 411–417.

Jung, H., and S.-I. Karato (2001), Water-induced fabric transitions in Olivine, *Science*, *293*, 1460–1463.

Li, A., and C. Chen (2006), Shear wave splitting beneath the central Tien Shan and tectonic implications, *Geophys. Res. Lett.*, *33*, L22303, doi:10.1029/2006GL027717.

Liu, H., P. M. Davis, and S. S. Gao (1995), SKS splitting beneath southern California, *Geophys. Res. Lett.*, *22*, 767–770.

Liu, K. H., S. S. Gao, Y. Gao, and J. Wu (2008), Shear-wave splitting and mantle flow associated with the deflected Pacific slab beneath northeast Asia, *J. Geophys. Res.*, *113*, B01305, doi:10.1029/2007JB005178.

Marone, F., and B. Romanowicz (2007), The depth distribution of azimuthal anisotropy in the continental upper mantle, *Nature*, *447*, 198–201.

McNamara, D. E., T. J. Owens, P. G. Silver, and F. T. Wu (1994), Shear wave anisotropy beneath the Tibetan Plateau, *J. Geophys. Res.*, *99*(B7), 13,655–13,665.

Ribe, N. M., and Y. Yu (1991), A theory for plastic deformation and textural evolution of olivine polycrystals, *J. Geophys. Res.*, *96*, 8325–8355.

Sandvol, E., J. Ni, S. Ozalaybey, and J. Schlue (1992), Shear-wave splitting in the Rio Grande Rift, *Geophys. Res. Lett.*, *19*, 2337–2340.

Savage, M. K. (1999), Seismic anisotropy and mantle deformation: what have we learned from shear wave splitting?, *Rev. Geophys.*, *37*(1), 65–106.

Silver, P. G. (1996), Seismic anisotropy beneath the continents—Probing the depths of geology, *Annu. Rev. Earth Planet. Sci.*, *24*, 385–432.

Silver, P. G., and W. W. Chan (1991), Shear wave splitting and subcontinental mantle deformation, *J. Geophys. Res.*, *96*, 16,429–16,454.

Silver, P. G., and W. E. Holt (2002), The mantle flow field beneath western North America, *Science*, *295*, 1054–1057.

Silver, P. G., and M. K. Savage (1994), The interpretation of shear-wave splitting parameters in the presence of two anisotropic layers, *Geophys. J. Int.*, *119*, 949–963.

Vecsey, L., J. Plomerova, and V. Babuska (2008), Shear-wave splitting measurements—Problems and solutions, *Tectonophysics*, *462*, 178–196.

Wang, C. Y., L. M. Flesch, P. G. Silver, L. J. Chang, and W. W. Chan (2008), Evidence for mechanically coupled lithosphere in central Asia and resulting implications, *Geology*, *36*, 363–366, doi:10.1130/G24450A.

Wolfe, C. J., and S. C. Solomon (1998), Shear-wave splitting and implications for mantle flow beneath the MELT region of the East Pacific Rise, *Science*, *22*, 1230–1232.

Zhang, S., and S. I. Karato (1995), Lattice preferred orientation of olivine aggregates deformed in simple shear, *Nature*, *375*, 774–777, doi:10.1038/375774a0.